Inorganic Chemistry

Article

pubs.acs.org/IC

Synthesis, Luminescence, and Energy-Transfer Properties of β-$Na_2Ca_4(PO_4)_2(SiO_4)$:A (A = Eu^{2+}, Dy^{3+}, Ce^{3+}/Tb^{3+}) Phosphors

Kai Li,[†,‡] Mengmeng Shang,[†] Dongling Geng,[†,‡] Hongzhou Lian,[†] Yang Zhang,[†,‡] Jian Fan,[†] and Jun Lin*[,†]

[†]State Key Laboratory of Rare Earth Resource Utilization, Changchun Institute of Applied Chemistry, Chinese Academy of Sciences, Changchun, 130022 Jilin P. R. China

[‡]University of the Chinese Academy of Sciences, Beijing 100049, P. R. China

Supporting Information

ABSTRACT: A series of β-$Na_2Ca_4(PO_4)_2(SiO_4)$ (β-NCPS):A (A = Eu^{2+}, Dy^{3+}, Ce^{3+}/Tb^{3+}) phosphors were prepared via a high-temperature solid-state reaction route. The X-ray diffraction, Fourier transform infrared, photoluminescence (PL), cathodoluminescence (CL) properties, fluorescent lifetimes, and absolute quantum yield were exploited to characterize the samples. Under UV radiation, the β-NCPS:Eu^{2+} phosphors present bright green emissions, and the β-NCPS:Ce^{3+} phosphors show strong blue emissions, which are attributed to their $4f^65d^1 \rightarrow 4f^7$ and 5d−4f allowed transitions, respectively. The β-NCPS:Ce^{3+}, Tb^{3+} phosphors display intense tunable color from blue to green and high absolute quantum yields (81% for β-NCPS:0.12Ce^{3+} and 83% for β-NCPS:0.12Ce^{3+}, 0.08Tb^{3+}) when excited at 365 nm. Simultaneously, the energy transfer from Ce^{3+} to Tb^{3+} ions is deduced from the spectral overlap between Ce^{3+} emission and Tb^{3+} excitation spectra and demonstrated by the change of emission spectra and decay lifetimes. Moreover, the energy-transfer mechanism from Ce^{3+} to Tb^{3+} ions is confirmed to be exchange interaction according to the discussion of expression from Dexter and Reisfeld. Under a low-voltage electron-beam excitation, the β-NCPS:A (A = Eu^{2+}, Dy^{3+}, Ce^{3+}/Tb^{3+}) phosphors exhibit their characteristic emissions, and the emission profiles of β-NCPS:Ce^{3+},Tb^{3+} phosphors are obviously different from those of the PL spectra; this difference might be ascribed to their different luminescence mechanisms. These results in PL and CL properties suggest that β-NCPS:A (A = Eu^{2+}, Dy^{3+}, Ce^{3+}/Tb^{3+}) phosphors are potential candidates for solid-state lighting and field-emission displays.

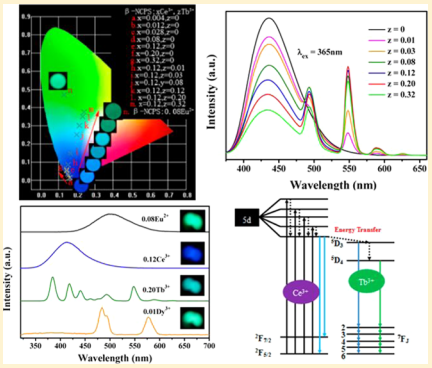

1. INTRODUCTION

Nowadays, white light-emitting diodes (wLEDs) and field-emitting displays (FEDs) have shown high potential as substitutes for traditional incandescent and implemented fluorescent lamps, as well as liquid-crystal displays (LCDs), by virtue of their respective special merits. As for wLEDs, they have the advantages of high efficiency, energy saving, environmental friendliness, long operation time, etc.[1] FEDs are potentially superior in lighting, viewing, operated-temperature range, power depletion, response time, and so on.[2] It is well-known that the phosphors are the key components in the process of wLED and FED fabrication; therefore, searching for proper novel phosphors that may potentially be applied to wLED and FED production has been a focused interest. It is well-accepted that introducing various rare earth ions into appropriate inorganic materials has been the most common route to achieve required phosphors, which are based on 4f−4f or 4f−5d transitions of rare earth ions.[3] Generally, the emission intensity of 4f−5d transitions are frequently strong due to their allowed characters, and these rare earth ions can act as direct activators, such as Eu^{2+}, Ce^{3+}, Sm^{2+}, etc. In addition, their luminescence colors can vary in different hosts due to the influence on the outermost 5d electronic shell by the crystal field.[4] In contrast, involving 4f−4f spin-forbidden transitions is usually not favorable for luminescence when excited at their f−f absorption areas because the 4f electronic shell is regularly shielded by the 5d electronic shell, and, therefore, these ions are minorly affected by a round crystal field, such as that in Tb^{3+}, Eu^{3+}, Dy^{3+}, etc.[5] Accordingly, the emission lines of visible emission spectra are narrow as well as characteristic, and the emission intensity is rather weak, which is not beneficial for full-spectra emitting and applications in phosphors. However, an effective method is to introduce a sensitizer (Eu^{2+} or Ce^{3+}) to transfer its absorption energy to the activator, which can greatly enhance the emission intensity of the activator, such as $Y_4Si_2O_7N_2$:Ce^{3+},Tb^{3+}, $SrZnP_2O_7$:Dy^{3+},Ce^{3+}, $(K_{1-x}Na_x)$-$SrPO_4$:Eu^{2+},Tb^{3+}, or $KCaY(PO_4)_2$:Ce^{3+},Tb^{3+}.[6]

Phosphate and silicate are often appropriate hosts for rare earth ions,[1a,4a,6b−d] and the luminescence properties of their phosphors are good; therefore, it is proposed that the performance of silicophosphate would be similar to those phosphors. The photoluminescence (PL) properties of Ce^{3+},Tb^{3+},Mn^{2+} doped $Ca_5(PO_4)_2(SiO_4)$ and Ce^{3+} doped

Received: March 10, 2014
Published: June 6, 2014

   dx.doi.org/10.1021/ic500545y | Inorg. Chem. 2014, 53, 6743−6751

$Sr_5(PO_4)_2(SiO_4)$[7] phosphors have been reported recently. However, there is no research on luminescence properties of rare earth ion doped β-$Na_2Ca_4(PO_4)_2(SiO_4)$. In this work, we prepare a series of novel luminescent materials with the chemical composition of β-$Na_2Ca_4(PO_4)_2(SiO_4)$ (abbreviated as β-NCPS):A (A = Eu^{2+}, Dy^{3+}, Ce^{3+}/Tb^{3+}). The PL and cathodoluminescence (CL) properties of these phosphors were investigated in detail, under, respectively, UV radiation and a low-voltage electron-beam excitation. The energy transfer from Ce^{3+} to Tb^{3+} ions greatly enhances the emission intensity of Tb^{3+}, and the energy-transfer mechanism from Ce^{3+} to Tb^{3+} ions is also discussed. On the basis of energy transfer, the emission color can be tuned from blue to green under UV excitation by adjusting the relative ratio of Ce^{3+} and Tb^{3+} concentrations in Ce^{3+},Tb^{3+}-codoped β-NCPS phosphors.

2. EXPERIMENT SECTION

2.1. Materials and Preparation. A series of β-NCPS:A (A = Eu^{2+}, Dy^{3+}, Ce^{3+}/Tb^{3+}) powder samples were synthesized by a high-temperature solid-state reaction process. The doping ions Eu^{2+}, Ce^{3+}, Tb^{3+}, and Dy^{3+}, all considered to substitute for Ca^{2+} in a β-NCPS host, were selected in concentrations of 1−32 mol %, 0.4−40 mol %, 1−60 mol %, and 0.3−16 mol %, respectively. Typically, stoichiometric amounts of Na_2CO_3 (analytical reagent (A.R.)), $CaCO_3$ (A.R.), SiO_2 (A.R.), $NH_4H_2PO_4$ (A.R.), and Eu_2O_3, CeO_2, Tb_4O_7, Dy_2O_3 (all >99.99%) were thoroughly mixed in an agate mortar for 35 min with an appropriate amount of ethanol and then dried at 80 °C for 1 h. After they were ground for 5 min once again, the powder mixtures were preheated at 800 °C for 4 h in a box furnace under air condition and then transferred to the tube furnace at 1200 °C for 5 h in a reducing atmosphere of H_2 (5%) and N_2 (95%) to produce the final samples, after they were reground for 3 min.

2.2. Measurement Characterization. The X-ray diffraction (XRD) patterns were performed on a D8 Focus diffractometer at a scanning rate of 10° min^{-1} in the 2θ range from 10° to 120° with graphite-monochromatized Cu Kα radiation (λ = 0.154 05 nm). Infrared spectra were collected on a VERTEX 70 Fourier transform infrared (FT-IR) spectrometer (Bruker). The PL and CL emission spectra were recorded with a Hitachi F-7000 spectrophotometer with different excitation sources (a 150 W xenon lamp and electron beam, respectively). The CL measurements were carried out in an ultrahigh vacuum chamber (<10^{-8} Torr) where the phosphors were excited by an electron beam in the voltage range of 2−6 kV and different filament currents (82−88 mA). The luminescence decay lifetimes were measured using a Lecroy Wave Runner 6100 Digital Osilloscope (1 GHz) with a tunable laser (pulse width = 4 ns, gate = 50 ns) as the excitation source (Contimuum Sunlite OPO). PL quantum yields (QYs) were obtained directly by the absolute PL quantum yield (internal quantum efficiency) measurement system (C9920−02, Hamamatsu Photonics K. K., Japan), including an excitation light source of a Xe lamp, a monochromator, an integrating sphere capable of nitrogen gas flow, and a CCD spectrometer for detecting the whole spectral range simultaneously. All the measurements were conducted at room temperature (RT).

3. RESULTS AND DISCUSSION

3.1. Phase Identification and Purity. The phase composition and purity of the as-prepared powder samples were detected by XRD first. Figure 1 shows the representative XRD patterns of β-NCPS host and Eu^{2+} or Ln^{3+} (Ln^{3+} = Ce^{3+}, Tb^{3+}, Dy^{3+}) doped β-NCPS samples. It is evident that the peaks in the patterns can be well-indexed to the pure β-$Na_2Ca_4(PO_4)_2(SiO_4)$ with JCPDS Card No. 32−1053; no other impurities were found, indicating the prepared samples were single phase. The Bragg diffraction 2θ at 22.96, 23.21, 32.44, 33.29, and 40.97° are represented to correspond to the indices

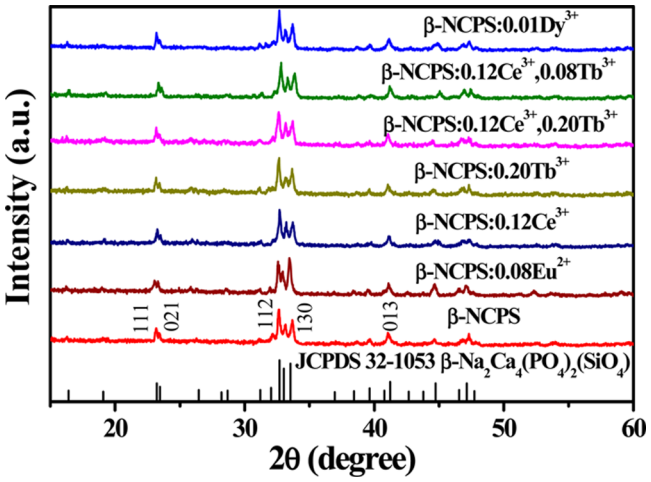

Figure 1. Representative XRD patterns of β-NCPS host and Eu^{2+} or Ln^{3+} doped β-NCPS samples synthesized at 1200 °C for 5 h. The reference is standard card data of β-$Na_2Ca_4(PO_4)_2(SiO_4)$ (JCPDS No. 32−1053).

of the crystallographic planes of (111), (021), (112), (130), and (013), respectively. The Eu^{2+} or Ln^{3+} ions were incorporated into hosts by replacing Ca^{2+} ions based on their similar ionic radii.[8] Moreover, their introductions into hosts did not arouse any significant change in the host structure. According to I. Kapralik's report,[9] the $Na_2Ca_4(PO_4)_2(SiO_4)$ phase has two kinds of crystal structures, called α and β, which are formed at higher and lower temperatures, respectively. The β-NCPS crystallizes in the orthorhombic space group *Pmcn* with cell parameters of a = 5.467(2) Å, b = 9.257(3) Å, c = 6.795(5) Å, and V = 343.88 $Å^3$, but, unfortunately, the number of chemical formula in the unit cell Z is not given; therefore, the specific structure can not be attained.

To identify the existence of orthophosphate in our synthesized samples, the FT-IR spectra were measured. Supporting Information, Figure S1 clearly displays the FT-IR spectra of representative β-NCPS host and Eu^{2+} and Ce^{3+}/Tb^{3+} doped samples. Generally, the IR absorption band of $(PO_4)^{3-}$ is located at 1120−940 cm^{-1} and 650−540 cm^{-1},[10] which includes the two absorption peaks observed at 1038 and 570 cm^{-1}, corresponding to the symmetric stretching mode of $(PO_4)^{3-}$ units. Another two peaks at 1975 and 3457 cm^{-1} are assigned to OH^- vibrations resulting from the covered water on the surface of phosphors under air condition.

3.2. Photoluminescence Properties. Figure 2a illustrates the PL emission spectra of β-NCPS:$n$$Eu^{2+}$ (n = 0.01−0.32) samples excited with 308 nm UV with varied concentrations of Eu^{2+} ions. Each broad emission band extends from 400 to 600 nm, with the full width at half-maximum of about 75 nm peaking at 494 nm, which is attributed to the $4f^65d^1 \rightarrow 4f^7$ allowed transition of Eu^{2+} ions. The emission wavelength range mainly covers the green area, which makes the phosphor show bright green color under a 365 nm UV lamp excitation (seen in the inset photograph). The PL excitation spectrum of a representative β-NCPS:0.08Eu^{2+} sample monitored at 494 nm is presented in Figure 2a, which includes the extent from 200 to 450 nm centered at 308 nm corresponding to the $4f^7$−$4f^65d^1$ transition of Eu^{2+}, matching well with UV-pumped $Ga_xAl_{1-x}N$ LED chips (the emission wavelength can extend to 300 nm). The optimal Eu^{2+} doping concentration x in this host is 0.08 here (seen from the dependence of emission intensity on Eu^{2+}

dx.doi.org/10.1021/ic500545y | Inorg. Chem. 2014, 53, 6743−6751

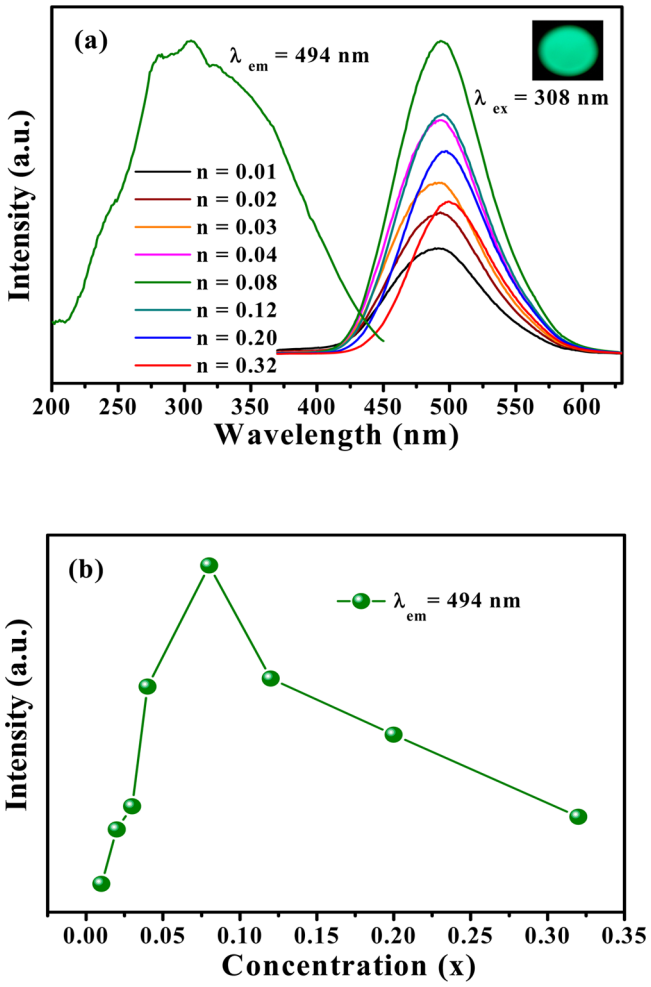

Figure 2. (a) PL emission spectra of β-NCPS:nEu^{2+} under an excitation of 308 nm UV and the PL excitation spectrum of β-NCPS:0.08Eu^{2+}. (b) Dependence of emission intensity on Eu^{2+} concentration n. (inset) Digital photograph of β-NCPS:0.08Eu^{2+} under a 365 nm UV lamp excitation.

concentration in Figure 2b), beyond which the emission intensities of phosphors start to decrease as a result of the concentration quenching effect. Usually, the concentration quenching of luminescence originates from the energy migration among the activator ions at high concentrations. Moreover, the slight red shift occurs with increasing Eu^{2+} concentration in this host; this shift may be attributed to the substitution of larger Eu^{2+} ions for smaller Ca^{2+} ions, resulting in a smaller distance between Eu^{2+} and O^{2-} ions, which would enhance the crystal field strength and lead to the red shift.[11]

To investigate the energy-transfer behavior among Eu^{2+} ions for concentration quenching, the linear fitting of log(n) versus log(I/n) in β-NCPS:nEu^{2+} phosphors beyond the quenching concentration is depicted in Figure 3. This behavior can be examined by the following expression proposed by Van Uitert, Ozawa, and Jaffe:[12]

$$\frac{I}{n} = [1 + \beta(n)^{\theta/3}]^{-1} \quad (1)$$

where I is the emission intensity, n is the activator ion concentration, which is not less than the critical value, and β is a constant for the same host crystal under the same excitation conditions. The type of nonradiative resonant energy transfer

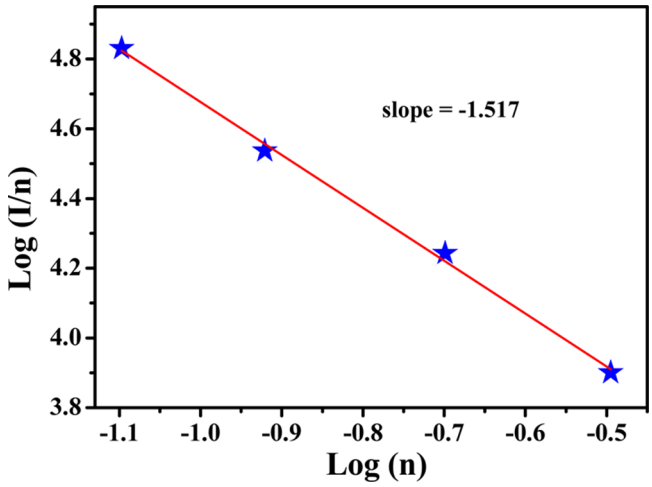

Figure 3. Linear fitting of log(n) vs log(I/n) for β-NCPS:nEu^{2+} phosphors, where I and n are the emission intensity and activator concentration, respectively.

can be estimated by analyzing the constant θ from this formula. The values of θ are 6, 8, and 10, corresponding to the energy-transfer mechanisms of electric dipole−dipole (d−d), dipole−quadrupole (d−q), or quadrupole−quadrupole (q−q) interactions, respectively. As illustrated in Figure 3, the slope of the fitting line is −1.517; therefore, the corresponding value of θ = 4.551 is close to 6,[13] which indicates the electric d−d interaction is the dominant mechanism in Eu^{2+} singly doped phosphors.

Upon 348 nm UV excitation, the emission spectrum of the β-NCPS:0.12Ce^{3+} phosphor exhibits a broad asymmetric band ranging from 370 to 570 nm, which is ascribed to the Ce^{3+} 5d^1 → 4f^1 allowed transition, as shown in Figure 4a. Generally, the band can be deconvoluted into two symmetric bands because of the spin−orbit splitting of the ground state ($^2F_{5/2}$ and $^2F_{7/2}$) with an energy difference of about 2000 cm^{-1}.[14] Herein, the energy difference between two fitting energy level (419 and 453 nm) gap is calculated to be 1791 cm^{-1}, which is consistent with theoretical value of 2000 cm^{-1}. Figure 4b shows the PL excitation spectrum of β-NCPS:0.12Ce^{3+} monitored at 425 nm and the dependence of luminescence properties of β-NCPS:xCe^{3+} (x = 0.004−0.40) phosphors on Ce^{3+} concentration. The excitation spectrum exhibits a broad band ranging from 200 to 400 nm centered at 284 and 348 nm, matching well with UV-pumped Ga$_x$Al$_{1-x}$N LED chips. The emission intensity of β-NCPS:0.12Ce^{3+} samples rises gradually with increasing Ce^{3+} concentration x and saturates when x = 0.12, beyond which the intensity begins to fall (seen from the variation of emission intensity in Figure 4c), and this is attributed to the conventional concentration quenching effect. We can clearly observe (in Supporting Information, Figure S2a) that the wavelengths of emission peaks occur a slight red shift from 414 (for x = 0.004) to 430 nm (for x = 0.40) as the increasing concentration of Ce^{3+} ion in β-NCPS hosts is excited at 348 nm. In addition, with the increasing excitation wavelength, the emission peaks of β-NCPS:0.12Ce^{3+} also show a similar red shift from 423 (λ_{ex} = 284 nm) to 441 nm (λ_{ex} = 380 nm) (see Supporting Information, Figure S2b). These two kinds of red shifts can be ascribed either to the reabsorption of Ce^{3+}, owing to the superior overlap between its emission and excitation spectra, or to the crystallinity that was

dx.doi.org/10.1021/ic500545y | Inorg. Chem. 2014, 53, 6743−6751

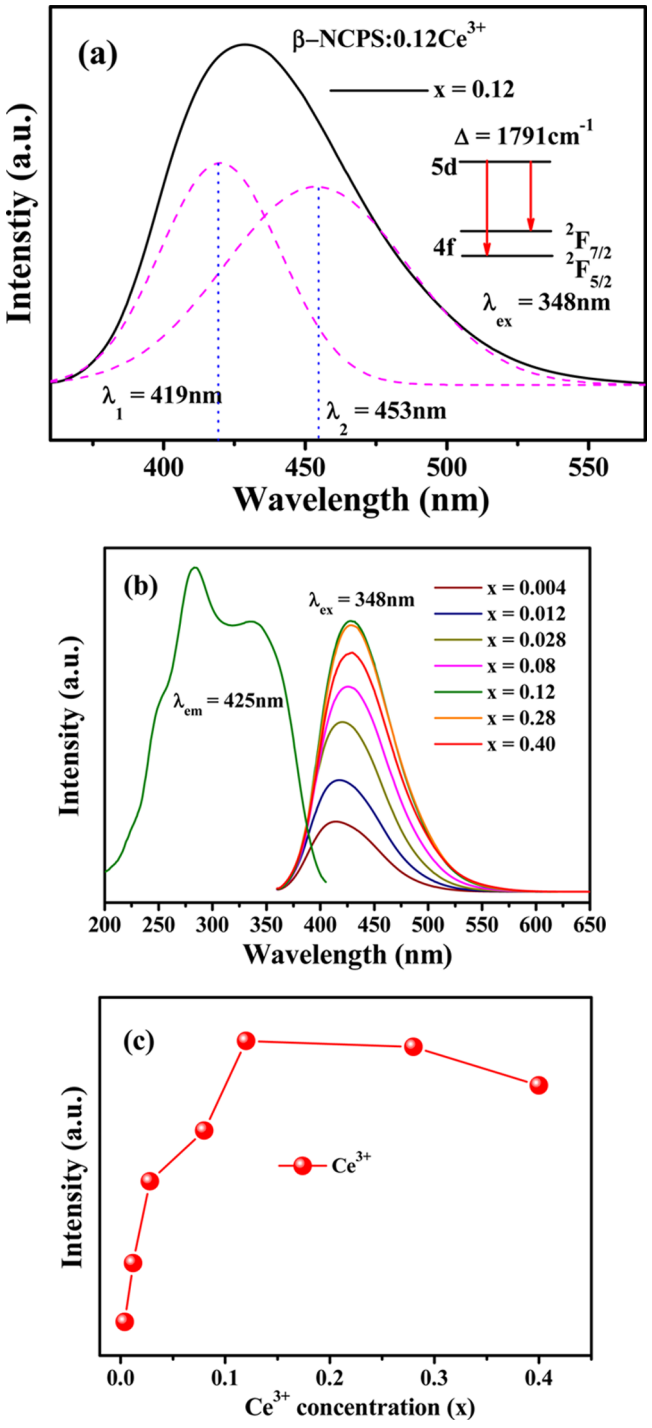

Figure 4. (a) Gaussian deconvolution of β-NCPS:0.12Ce^{3+} emission excited at 348 nm. (b) PL emission spectra in β-NCPS:$x$$Ce^{3+}$ (x = 0.004−0.40) phosphors with different Ce^{3+} concentration excited at 348 nm and PL excitation spectrum of β-NCPS:0.12Ce^{3+} phosphor monitored at 425 nm. (c) The variation of Ce^{3+} emission intensity as a function of Ce^{3+} concentration x.

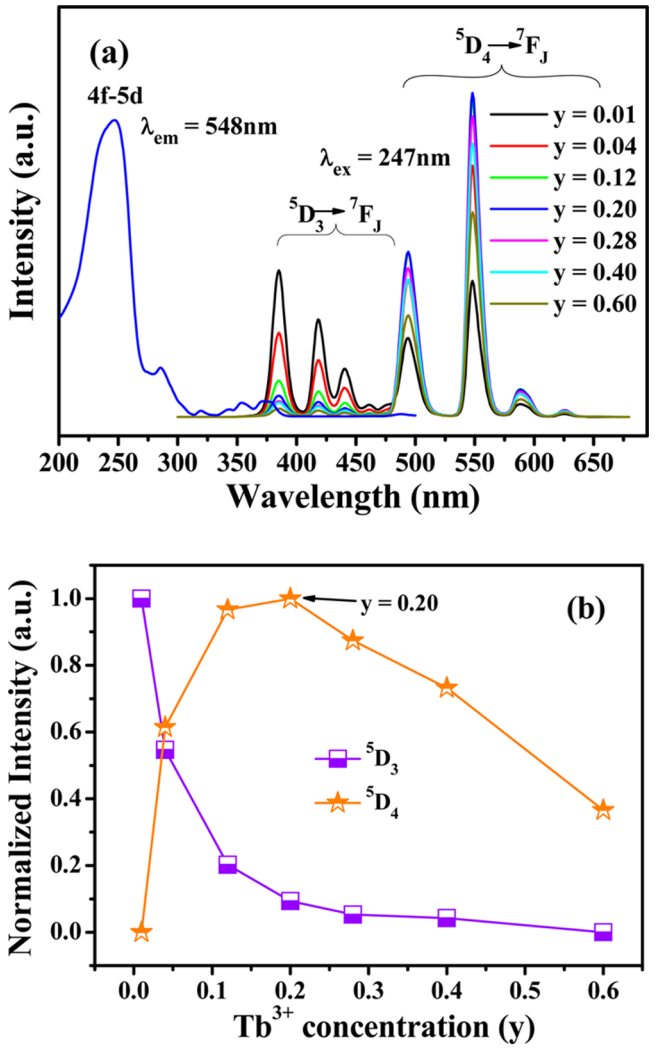

Figure 5. (a) PL emission spectra for β-NCPS:$y$$Tb^{3+}$ (y = 0.01−0.60) phosphors with different concentration of Tb^{3+} excited at 247 nm and excitation spectrum for β-NCPS:0.20Tb^{3+} sample monitored at 548 nm. (b) Dependence of emission intensities of $^5D_3$ and $^5D_4$ in β-NCPS:$y$$Tb^{3+}$ phosphors on Tb^{3+} concentration y.

worsened by higher Ce^{3+} concentrations in the doped β-NCPS[15] (see Supporting Information, Figure S2c).

As an important activator, the Tb^{3+} ion has been investigated in detail in many hosts.[16] For the β-NCPS host also, the Tb^{3+} ion can be well-incorporated into the crystal lattice as an effective activator. Figure 5a represents a PL excitation spectrum for the β-NCPS:0.20Tb^{3+} sample monitored at its characteristic green emission peak (548 nm) and the variation of PL emission spectra for β-NCPS:$y$$Tb^{3+}$ (y = 0.01−0.60) phosphors with varied concentrations of the Tb^{3+} ion excited at 247 nm. The excitation spectrum contains many peaks in the region of 200−500 nm, which refers to a wide band centered at 247 nm resulting from its 4f−5d allowed transition and other excitation lines at 286, 319, 343, 354, 372, and 489 nm corresponding to absorption of its 4f−4f spin-forbidden transitions. Upon 247 nm excitation, the emission spectrum of β-NCPS:0.20Tb^{3+} consists of the $^5D_{3,4}$−$^7F_{J(J=6,5,4,3,2)}$ transitions of Tb^{3+} ions, which covers the blue emission from the $^5D_3$ level and the green emission from the $^5D_4$ level. The energy difference between the $^5D_3$ and $^5D_4$ levels is close to that between those of $^7F_6$ and $^7F_0$, which usually leads to cross-relaxation by the resonant energy-transfer process: $^5D_3$ (Tb^{3+}) + $^7F_6$ (Tb^{3+}) − $^5D_4$ (Tb^{3+}) + $^7F_0$ (Tb^{3+}).[16] As exhibited in Figure 5b, upon excitation at 247 nm, the emission intensity of $^5D_3$ monotonously decreases with the increase of Tb^{3+} concentration, while for $^5D_4$, the emission intensity first rises and then descends after a maximum when y = 0.20 because of the usual concentration quenching effect.

dx.doi.org/10.1021/ic500545y | Inorg. Chem. 2014, 53, 6743−6751

3.3. Energy Transfer in β-NCPS:0.12Ce^{3+},zTb^{3+} Phosphors. The emission intensity of Tb^{3+} is usually weak when the excitation wavelength is located in the f−f transition area of that ion.[17] It is commendable to introduce a Ce^{3+} or Eu^{2+} to enhance its emission intensity via energy transfer.[18,16c] The spectral overlap between Ce^{3+} PL emission spectra and Tb^{3+} PL excitation spectrum is presented, for this host, in Supporting Information, Figure S3. This overlap indicates the possibility of energy transfer from Ce^{3+} to Tb^{3+} ions, which would result in the enhancement of Tb^{3+} emission.

As depicted above, when Ce^{3+} and Tb^{3+} ions are codoped into the β-NCPS host, the energy transfer from Ce^{3+} to Tb^{3+} ions is expected to occur when excited by UV radiation. Figure 6a shows the variation of PL emission spectra excited at 365 nm

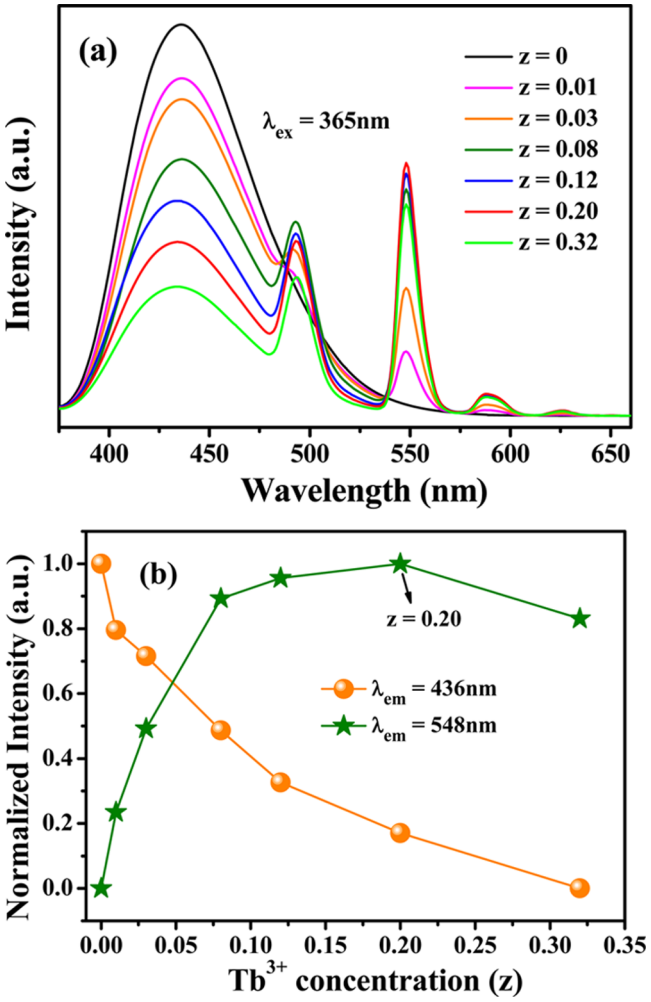

Figure 6. (a) Emission spectra of β-NCPS:0.12Ce^{3+},zTb^{3+} (z = 0–0.32) phosphors with different Tb^{3+} content z. (b) Variation of emission intensity as a function of Tb^{3+} content z with fixed Ce^{3+} concentration.

in β-NCPS:0.12Ce^{3+},zTb^{3+} (z = 0–0.32) phosphors with different Tb^{3+} content z. This variation consists of the emission bands of both Ce^{3+} and Tb^{3+} ions. With rising Tb^{3+} concentration, one finds the emission intensity of Ce^{3+} ions (at 436 nm) monotonously decreases, while Tb^{3+} emission intensity (at 548 nm) first obviously increases to a maximum when z = 0.20 and then declines due to the concentration quenching effect, which can be directly observed in Figure 5b. This result confirms the energy transfers from Ce^{3+} to Tb^{3+} ions.

To further certify the energy transfer from Ce^{3+} to Tb^{3+} ions in this host, the PL decay curves of Ce^{3+} in β-NCPS:0.12Ce^{3+},zTb^{3+} with varying concentrations of the Tb^{3+} ion are obtained for the Ce^{3+} emission at 436 nm (λ_{ex} = 300 nm) (see Supporting Information, Figure S4). The decay behaviors of Ce^{3+} ions in all the representative samples fit well with single-exponential rule, which can be evaluated by the following equation:[19]

$$I = I_0 \exp\left(\frac{-t}{\tau}\right) \quad (2)$$

Here, I and I_0 represent the luminescence intensity at times t and 0, respectively, and τ is the calculated decay lifetime. From eq 2, the effective lifetimes in β-NCPS:0.12Ce^{3+},zTb^{3+} samples are determined to be 50.21, 45.92, 43.93, 41.63, 39.21, and 34.45 ns, corresponding to z = 0, 0.01, 0.04, 0.08, 0.16, and 0.32, respectively. The monotonous drop of lifetimes of Ce^{3+} with increasing Tb^{3+} concentration further proves the existence of energy transfer from Ce^{3+} to Tb^{3+} ions.

With respect to this host, the energy-transfer efficiency η_T from Ce^{3+} to Tb^{3+} ions in β-NCPS:0.12Ce^{3+},zTb^{3+} phosphors can be acquired by the earlier given equation:[20]

$$\eta_T = 1 - \frac{I_S}{I_{S0}} \quad (3)$$

where η_T is the energy-transfer efficiency and I_{S0} and I_S are the luminescence intensities of Ce^{3+} ions in the absence and presence of Tb^{3+} ions, respectively. As seen in Figure 7, the

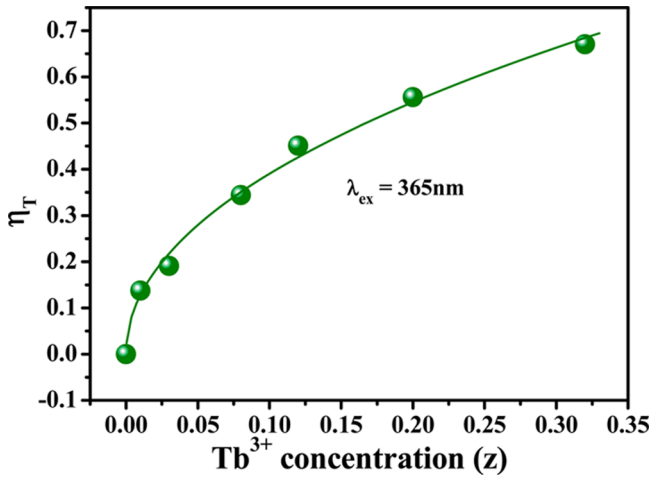

Figure 7. Dependence of η_T on Tb^{3+} ion concentration z in β-NCPS:0.12Ce^{3+},zTb^{3+} (z = 0–0.32) samples.

energy-transfer efficiency monotonously ascends (0.14, 0.19, 0.34, 0.45, 0.56, and 0.67, corresponding to z = 0.01, 0.03, 0.08, 0.12, 0.20, and 0.32, respectively) with constantly increasing Tb^{3+} concentration, while the rate of increase decreases because the fixed Ce^{3+} content limits the further energy transfer from Ce^{3+} to Tb^{3+} ions.

On the basis of Dexter's energy-transfer expression of multipolar interaction and Reisfeld's approximation, the energy-transfer behavior from Ce^{3+} to Tb^{3+} ions can take place via exchange interaction and electric-multipole interactions. The following formula can be adopted:[21]

dx.doi.org/10.1021/ic500545y | Inorg. Chem. 2014, 53, 6743−6751

$$\frac{\eta_0}{\eta} \propto C^{\alpha/3} \tag{4}$$

where η_0 and η are the luminescence quantum efficiencies of Ce^{3+} in the absence and presence of Tb^{3+}, respectively; C is the total concentration of Ce^{3+} and Tb^{3+} ions; and the α values of 3, 6, 8, and 10 correspond to exchange interaction, d−d, d−q, and q−q interactions, respectively. To carry out a simple evaluation, the value of η_0/η can be estimated by the luminescence intensity ratio (I_{S0}/I_S) as follows:

$$\frac{I_{S0}}{I_S} \propto C^{\alpha/3} \tag{5}$$

where I_{S0} and I_S are the emission intensities of Ce^{3+} in the absence and presence of Tb^{3+}, respectively. The least-squares fittings of I_{S0}/I_S versus $C^{\alpha/3}_{Ce^{3+}+Tb^{3+}}$ (α = 3, 6, 8, 10, respectively), as exhibited in Figure 8, illustrate that the linear relationship of

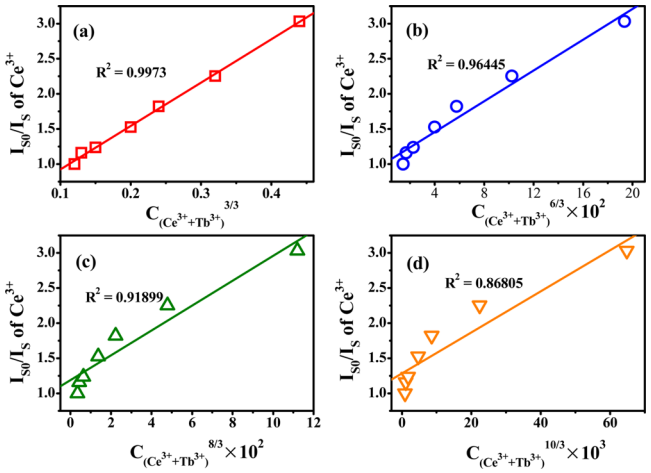

Figure 8. Dependence of I_{S0}/I_S of Ce^{3+} on $C_{(Ce^{3+}+Tb^{3+})}$ (a), $C^{6/3}_{(Ce^{3+}+Tb^{3+})}$ (b), $C^{8/3}_{(Ce^{3+}+Tb^{3+})}$ (c), and $C^{10/3}_{(Ce^{3+}+Tb^{3+})}$ (d).

exchange interaction is the best one among the fitting results, implying that energy transfer from Ce^{3+} to Tb^{3+} ions in the β-NCPS host is dominated by the exchange interaction, which is identical to that in $Ca_2Al_3O_6F$:Ce^{3+},Tb^{3+} phosphors.[21b]

The CIE chromaticity coordinates of synthesized samples β-NCPS:0.08Eu^{2+} excited at 308 nm and β-NCPS:$x$$Ce^{3+}$,$z$$Tb^{3+}$ with different Ce^{3+}/Tb^{3+} doped concentrations excited at 365 nm are gained from Supporting Information, Table S1. Moreover, the variety can be seen from Figure 9, where a−g represent the variation of Ce^{3+} concentration singly doped samples and h−m show the change of different Tb^{3+} content with stationary Ce^{3+} concentration in β-NCPS:0.12Ce^{3+},$z$$Tb^{3+}$ samples. It appears green (0.131, 0.471) for β-NCPS:0.08Eu^{2+} (represented by n) and tunable color from blue (0.146, 0.050) to green (0.239, 0.374) for β-NCPS:0.12Ce^{3+},$z$$Tb^{3+}$ with increasing Tb^{3+} concentration z from 0 to 0.32. This is also easily observed via the photographs of luminescent phosphors excited under a 365 nm UV lamp in Figure 9. The QYs can be determined by the integrated sphere method,[22,7a] which is obtained by the following equation:

$$\eta = \frac{E_i(\lambda) - (1 - A)E_0(\lambda)}{L_e(\lambda)A} \tag{6}$$

where $E_i(\lambda)$ is the integrated luminescence upon direct excitation, and $E_0(\lambda)$ is the integrated luminescence excited

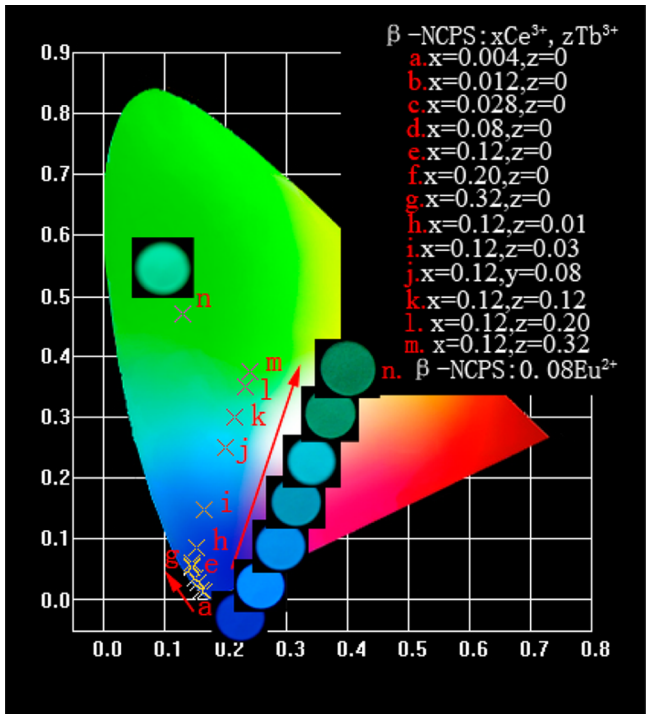

Figure 9. CIE chromaticity coordinates of β-NCPS:0.08Eu^{2+} excited at 308 nm, β-NCPS:$x$$Ce^{3+}$, $z$$Tb^{3+}$ (x = 0.004−0.32, z = 0−0.32) with different Ce^{3+}/Tb^{3+} doped concentrations under 365 nm excitation. The digital photographs of representative samples were taken under a 365 nm UV lamp excitation.

by indirect illumination from the integrated sphere. The value $L_e(\lambda)$ is the integrated excitation profile acquired from the empty integrated sphere (absence of sample). The optical absorbance A can be gained via using the following formula:

$$A = \frac{L_0(\lambda) - L_i(\lambda)}{L_0(\lambda)} \tag{7}$$

where $L_0(\lambda)$ is the integrated excitation profile when the sample is diffusely illuminated by the integrated sphere's surface, and $L_i(\lambda)$ is the integrated excitation profile when the sample is directly excited by the incident beam. The corresponding value of different phosphors are displayed in Table 1, which shows the highest value is 27% for β-NCPS:0.04Eu^{2+} excited at 308 nm and 81% for β-NCPS:0.12Ce^{3+}, which is better than that of $NaSrBO_3$:Ce^{3+},[22] as well as 83% for β-NCPS:0.12Ce^{3+},0.08Tb^{3+}

Table 1. Quantum Yields (QYs) of β-NCPS:$n$$Eu^{2+}$ Excited at 308 nm, and β-NCPS:$x$$Ce^{3+}$, β-NCPS:0.12Ce^{3+},$z$$Tb^{3+}$ Excited at 365 nm

λ_{ex} = 308 nm		λ_{ex} = 365 nm			
β-NCPS:$n$$Eu^{2+}$		β-NCPS:$x$$Ce^{3+}$		β-NCPS:0.12Ce^{3+}, zT-b^{3+}	
n	QY(%)	x	QY(%)	z	QY(%)
0.01	8	0.004	10	0	81
0.02	24	0.012	14	0.01	76
0.03	22	0.028	31	0.03	80
0.04	27	0.08	47	0.08	83
0.08	21	0.12	81	0.12	69
0.12	13	0.20	72	0.20	66
0.28	5	0.32	67	0.32	59

dx.doi.org/10.1021/ic500545y | Inorg. Chem. 2014, 53, 6743−6751

excited at 365 nm. This indicates that the β-NCPS:nEu^{2+}, β-NCPS:xCe^{3+}, and β-NCPS:Ce^{3+},Tb^{3+} phosphors may have potential applications in wLEDs with the development of chips for wLEDs from 350 to 420 nm to shorter wavelength because the excitation spectra are rather broad, ranging from 200 to 400 nm.

3.4. Cathodoluminescence Properties. Additionally, the CL properties of as-synthesized β-NCPS:Eu^{2+}, Ce^{3+}, Tb^{3+}, and Dy^{3+} samples were investigated to recognize their potential application in FEDs. Figure 10 shows the typical CL spectra as

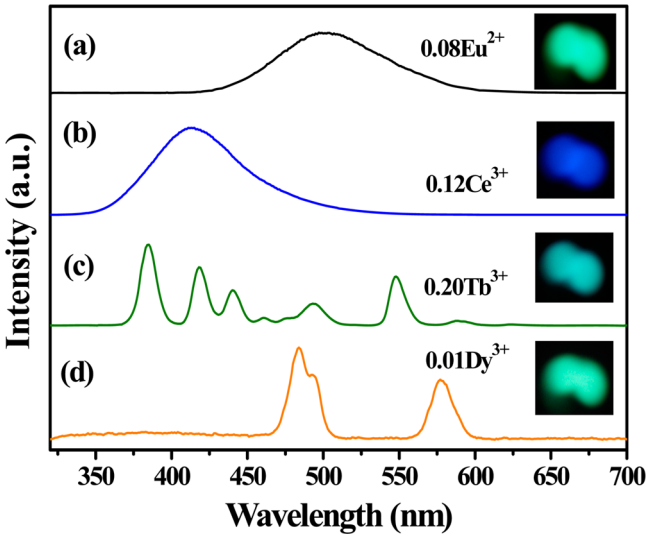

Figure 10. CL spectra for β-NCPS:0.08Eu^{2+} (a), β-NCPS:0.12Ce^{3+} (b), β-NCPS:0.20Tb^{3+} (c), and β-NCPS:0.01Dy^{3+} (d). (insets) The corresponding digital luminescence photographs under low-voltage electron-beam excitation.

well as corresponding luminescence photographs of β-NCPS:Eu^{2+}, Ce^{3+}, Tb^{3+}, and Dy^{3+} samples under low-voltage electron-beam bombardment. The CL spectra are similar to their PL spectra, but they are not the same, which may be due to the different excitation sources of low-voltage electron beam and Xe lamp. For the β-NCPS:0.20Tb^{3+} sample, the relative intensity of emission peaks at 380 and 548 nm in the CL spectrum is distinguished from that in the PL spectrum in Figure 5a. The β-NCPS:0.01Dy^{3+} sample has the characteristic emission peaks at 484 and 577 nm, and the peak at 495 nm is a bit different from its PL spectrum.

Figure 11a shows the CL spectra for β-NCPS:0.12Ce^{3+},zTb^{3+} (z = 0–0.24) phosphors under low-voltage electron-beam bombardment. The shape of the CL spectra is clearly different from that of the PL emission spectra; this difference can be ascribed to their different luminescence mechanisms.[3c,14a] Under UV excitation, the activator Ce^{3+} electrons can be excited to the 5d energy level and then radiatively transited to the 4f level via releasing a photon or via transferring their energy to nearby Tb^{3+} ions. Therefore, the emission intensity ratio of Ce^{3+} to Tb^{3+} ions depends on the energy-transfer efficiency from Ce^{3+} to Tb^{3+} ions. For CL, the primary fast electrons produce many secondary electrons. These secondary electrons excite the matrix lattice and create many electron–hole pairs, which can induce the formation of bound excitons. These excitons decay nonradiatively via a resonant or quasiresonant transfer from the Ce^{3+} to the Tb^{3+} ions simultaneously and give their characteristic emission.[23,14a]

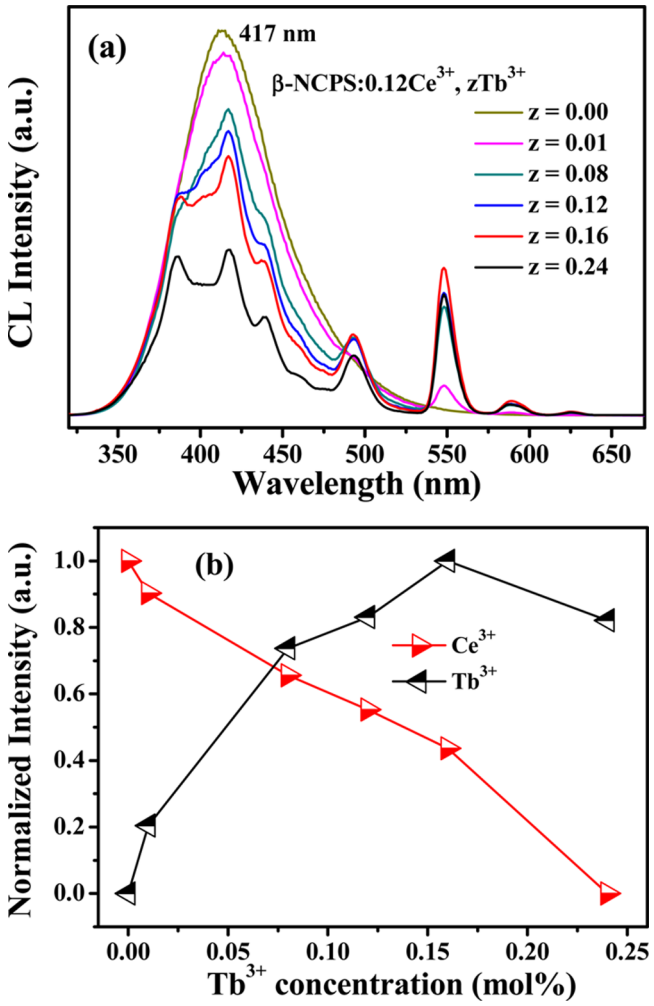

Figure 11. (a) CL spectra for β-NCPS:0.12Ce^{3+},zTb^{3+} (z = 0–0.24). (b) Variation of relative emission intensity for Ce^{3+} and Tb^{3+} ions.

Accordingly, the Ce^{3+} emission intensity falls, and the Tb^{3+} emission intensity first increases to a maximum when z = 0.16 and then decreases with increasing Tb^{3+} concentration (see Figure 11b).

The β-NCPS:0.08Eu^{2+}, β-NCPS:0.12Ce^{3+}, β-NCPS:0.20Tb^{3+}, and β-NCPS:0.12Ce^{3+},0.16Tb^{3+} samples were selected to investigate the relationship between emission intensity and the filament current as well as the accelerating voltage (see Figure 12). At a fixed accelerating voltage of 3.5 kV, the emission intensity monotonously increases with the increase of filament current from 80 to 88 mA. Similarly, the emission intensity monotonously rises with the increase of accelerating voltage from 2 to 6 kV at fixed filament current of 88 mA. And there is no conspicuous saturation observed for CL at this range of filament current and the accelerating voltage. These phenomena can be due to the deeper penetration of the electrons into the phosphor body and the larger electron-beam current density with the increase of filament current or accelerating voltage.

4. CONCLUSION

In summary, novel β-NCPS:Eu^{2+}, Dy^{3+}, and Ce^{3+}/Tb^{3+} phosphors were prepared via a high-temperature solid-state reaction route. Upon UV excitation, the β-NCPS:Eu^{2+} phosphors present bright green color emissions (400–600

dx.doi.org/10.1021/ic500545y | Inorg. Chem. 2014, 53, 6743–6751

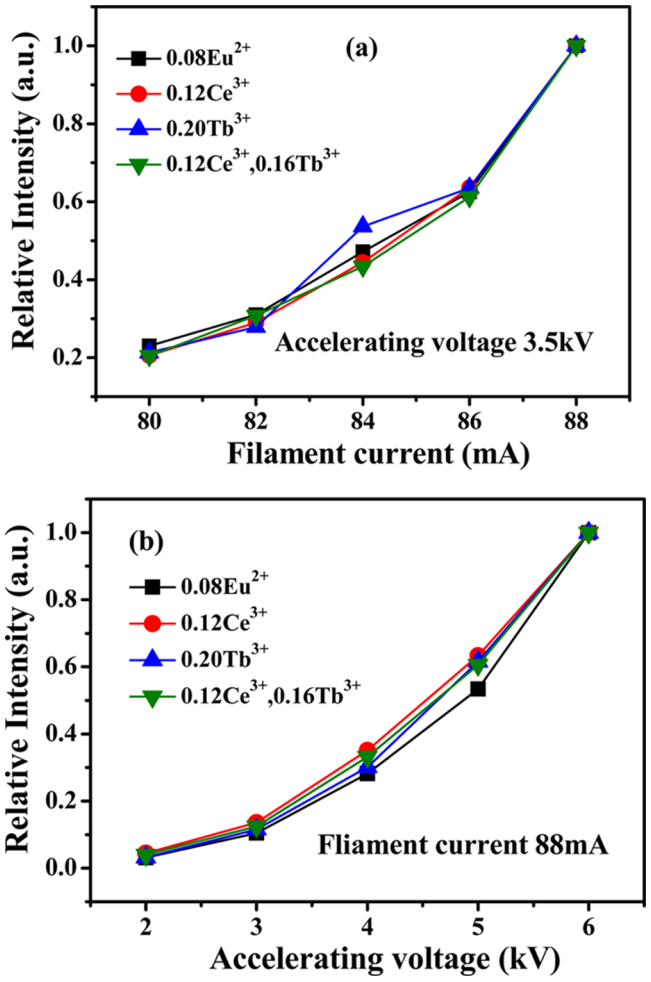

Figure 12. CL intensities of β-NCPS:0.08Eu^{2+}, β-NCPS:0.12Ce^{3+}, β-NCPS:0.20Tb^{3+}, and β-NCPS:0.12Ce^{3+},0.16Tb^{3+} as a function of filament current (a) and accelerating voltage (b).

nm) with peaks centered at about 494 nm. The β-NCPS:Ce^{3+} phosphors exhibit intense blue emissions, and their best quantum yield can reach 81% for β-NCPS:0.12Ce^{3+}, under 365 nm UV excitation. On the basis of cross-relaxation from $^5D_3$ to $^5D_4$, Tb^{3+} singly doped β-NCPS samples display light blue to cyan and then green color with the increase of its dopant concentration. When Ce^{3+} ions were codoped into β-NCPS:Tb^{3+} hosts, the intensive tunable luminescence was realized from blue to green by adjusting Tb^{3+} concentration, with the maximum quantum efficiency of 83% for β-NCPS:0.12Ce^{3+},0.08Tb^{3+} upon 365 nm UV excitation. The energy transfer from Ce^{3+} to Tb^{3+} ions is deduced via spectral overlap between the Ce^{3+} PL emission spectra and a Tb^{3+} PL excitation spectrum, then confirmed by the variation of emission spectra as well as the reduction of Ce^{3+} decay lifetimes with increasing Tb^{3+} concentration. Additionally, the CL of β-NCPS:Eu^{2+}, Dy^{3+}, and Ce^{3+}/Tb^{3+} phosphors were measured under low-voltage electron-beam bombardment, and their characteristic luminescence was obtained. With the increase of filament current or accelerating voltage, the CL emission intensity consecutively increases without saturation. Generally, these results indicate that β-NCPS:Eu^{2+}, Dy^{3+}, and Ce^{3+}/Tb^{3+} phosphors show promise as candidates for UV-pumped wLEDs and FEDs.

■ ASSOCIATED CONTENT

Supporting Information

This includes FT-IR spectra of the β-NCPS host and as-prepared representative phosphors (Figure S1), the red shift of photoluminescence emission spectra in β-NCPS:$x$$Ce^{3+}$ samples excited at 348 nm and in β-NCPS:0.12Ce^{3+} phosphor with different excitation wavelengths (Figure S2), the spectral overlap between Ce^{3+} emission and excitation spectra in β-NCPS:0.12Ce^{3+} phosphor, the spectral overlap between β-NCPS:0.12Ce^{3+} PL emission spectra and β-NCPS:0.20Tb^{3+} PLE spectrum (Figure S3), the PL decay curves for β-NCPS:0.12Ce^{3+},$z$$Tb^{3+}$ with different concentrations of Tb^{3+} ion (Figure S4), the CIE coordinates of β-NCPS:$n$$Eu^{2+}$ excited with 308 nm UV and β-NCPS:$x$$Ce^{3+}$ and β-NCPS:0.12Ce^{3+},$z$$Tb^{3+}$ excited with 365 nm UV (Table S1). This material is available free of charge via the Internet at http://pubs.acs.org.

■ AUTHOR INFORMATION

Corresponding Author

*E-mail: jlin@ciac.ac.cn.

Notes

The authors declare no competing financial interest.

■ ACKNOWLEDGMENTS

This project is financially supported by the National Natural Science Foundation of China (NSFC 51332008, 51172227, 21221061), the Joint Funds of the National Natural Science Foundation of China and Guangdong Province (U1301242), and the National Basic Research Program of China (2010CB327704, 2014CB643803).

■ REFERENCES

(1) (a) Jang, H. S.; Yang, H.; Kim, S. W.; Han, J. Y.; Lee, S. G.; Jeon, D. Y. *Adv. Mater.* **2008**, *20*, 2696−2702. (b) Piao, X.; Machida, K.; Horikawa, T.; Hanzawa, H.; Shimomura, Y.; Kijima, N. *Chem. Mater.* **2007**, *19*, 4592−4599. (c) Yeh, C. W.; Chen, W. T.; Liu, R. S.; Hu, S.; Sheu, H. S.; Chen, J. M.; Hintzen, H. T. *J. Am. Chem. Soc.* **2012**, *134*, 14108−14117. (d) Guo, N.; Zheng, Y.; Jia, Y.; Qiao, H.; You, H. *J. Phys. Chem. C* **2012**, *116*, 1329−1334. (e) Im, W. B.; Fellows, N. N.; DenBaars, S. P.; Seshadri, R.; Kim, Y. *Chem. Mater.* **2009**, *21*, 2957−2966. (f) Ci, Z.; Que, M.; Shi, Y.; Zhu, G.; Wang, Y. *Inorg. Chem.* **2014**, *53* (4), 2195−2199.

(2) (a) Liu, T. C.; Kominami, H.; Greer, H. F.; Zhou, W.; Nakanishi, Y.; Liu, R. S. *Chem. Mater.* **2012**, *24*, 3486−3492. (b) Shang, M.; Geng, D.; Zhang, Y.; Li, G.; Yang, D.; Kang, X.; Lin, J. *J. Mater. Chem.* **2012**, *22*, 19094−19104. (c) Zhang, N.; Guo, C.; Jing, H. *RSC Adv.* **2013**, *3*, 7495−7502. (d) Geng, D.; Shang, M.; Yang, D.; Zhang, Y.; Cheng, Z.; Lin, J. *J. Mater. Chem.* **2012**, *22*, 23789−23798.

(3) (a) Tu, D.; Liang, Y.; Liu, R.; Cheng, Z.; Yang, F.; Yang, W. *J. Alloys Compd.* **2011**, *509*, 5596−5599. (b) Zhang, Z.; Mao, Z.; Song, S.; Zhang, J.; Liu, L.; Zhang, W.; Wang, D. *Mater. Lett.* **2013**, *90*, 1−3. (c) Geng, D.; Li, G.; Shang, M.; Peng, C.; Zhang, Y.; Cheng, Z.; Lin, J. *Dalton Trans.* **2012**, *41*, 3078−3086. (d) Sun, J.; Lian, Z.; Shen, G.; Shen, D. *RSC Adv.* **2013**, *3*, 18395−18405. (e) Lü, W.; Zhang, X.; Wang, Y.; Hao, Z.; Liu, Y.; Luo, Y.; Wang, X.; Zhang, J. *J. Alloys Compd.* **2012**, *513*, 430−435.

(4) (a) Jang, H. S.; Jeon, D. Y. *Appl. Phys. Lett.* **2007**, *90*, 041906. (b) Yang, M.; Liu, L.; Chen, F. *Mater. Lett.* **2012**, *88*, 116−118. (c) Chiu, Y. C.; Liu, W. R.; Chang, C. K.; Liao, C. C.; Yeh, Y. T.; Jang, S. M.; Chen, T. M. *J. Mater. Chem.* **2010**, *20*, 1755−1758. (d) Song, H. J.; Yim, D. K.; Cho, I. S.; Roh, H. S.; Kim, J. S.; Kim, D. W.; Hong, K. S. *Mater. Res. Bull.* **2012**, *47*, 4522−4526. (e) Zhang, J.; Zhang, X.; Gong, M.; Shi, J.; Yu, L.; Rong, C.; Lian, S. *Mater. Lett.* **2012**, *79*, 100−102. (f) Wang, J.; Li, Y.; Huang, Y.; Shi, L.; Seo, H. J. *Mater. Chem.*

Phys. **2010**, *120*, 598−602. (g) Huang, Y.; Zhao, W.; Shi, L.; Seo, H. J. *J. Alloys Compd.* **2009**, *477*, 936−940.
(5) (a) Yerpude, A. N.; Dhoble, S. J. *J. Lumin.* **2012**, *132*, 2975−2978. (b) Ma, Q.; Lu, M.; Yuan, Z.; Zhu, Y.; Yang, P. *Mater. Res. Bull.* **2012**, *47*, 4126−4130. (c) Zhang, L.; Zhou, X.; Zeng, H.; Chen, H.; Dong, X. *Mater. Lett.* **2008**, *62*, 2539−2541. (d) Lakshminarasimhan, N.; Varadaraju, U. V. *Mater. Res. Bull.* **2008**, *43*, 2946−2953.
(6) (a) Xia, Z.; Wu, W. *Dalton Trans.* **2013**, *42*, 12989−12997. (b) Kohale, R. L.; Dhoble, S. J. *J. Alloys Compd.* **2014**, *586*, 314−318. (c) Dai, P.; Zhang, X.; Bian, L.; Lu, S.; Liu, Y.; Wang, X. *J. Mater. Chem. C* **2013**, *1*, 4570−4576. (d) Jiang, T.; Yu, X.; Xu, X.; Yu, H.; Zhou, D.; Qiu, J. *Mater. Res. Bull.* **2014**, *51*, 80−84.
(7) (a) Geng, D.; Shang, M.; Zhang, Y.; Lian, H.; Cheng, Z.; Lin, J. *J. Mater. Chem. C* **2013**, *1*, 2345−2353. (b) Tao, Z.; Huang, Y.; Seo, H. J. *Dalton Trans.* **2013**, *42*, 2121−2129.
(8) (a) Li, Y.; Deng, D.; Wang, Q.; Li, G.; Hua, Y.; Jia, G.; Huang, L.; Zhao, S.; Wang, H.; Li, C.; Xu, S. *J. Lumin.* **2012**, *132*, 1179−1182. (b) Shinde, K. N.; Dhoble, S. J.; Kumar, A. *Phys. B* **2011**, *406*, 94−99. (c) Geng, D.; Shang, M.; Zhang, Y.; Cheng, Z.; Lin, J. *Eur. J. Inorg. Chem.* **2013**, 2947−2953. (d) Grandhe, B. K.; Bandi, V. R.; Jang, K.; Kim, S. S.; Shi, D. S.; Lee, Y.; Lim, J. M.; Song, T. *J. Alloys Compd.* **2011**, *509*, 7937−7942.
(9) Kapralik, I.; Hanic, F. *Trans. Br. Ceram. Soc.* **1977**, *76*, 126−133.
(10) (a) Dillip, G. R.; Raju, B. D. P. *J. Alloys Compd.* **2012**, *540*, 67−74. (b) Zhu, G.; Ci, Z.; Shi, Y.; Que, M.; Wang, Q.; Wang, Y. *J. Mater. Chem. C* **2013**, *1*, 5960−5969. (c) Popovíc, L.; Waal, D.; J. Boeyens, C. A. *J. Raman Spectrosc.* **2005**, *36*, 2−11.
(11) Wen, D.; Dong, Z.; Shi, J.; Gong, M.; Wu, M. *ECS J. Solid State Sci. Technol.* **2013**, *2* (9), R178−185.
(12) (a) Ozawa, L.; Jaffe, P. M. *J. Electrochem. Soc.* **1967**, *114*, 1048−1053. (b) Xia, Z.; Liu, H.; Li, X.; Liu, C. *Dalton Trans.* **2013**, *42*, 16588−16595. (c) Song, H. J.; Yim, D. K.; Roh, H. S.; Cho, I. S.; Kim, S. J.; Jin, Y. H.; Shim, H. W.; Kim, D. W.; Hong, K. S. *J. Mater. Chem. C* **2013**, *1*, 500−505.
(13) (a) Chiu, Y. C.; Huang, C. H.; Lee, T. J.; Liu, W. R.; Yeh, Y. T.; Jang, S. M.; Liu, R. S. *Opt. Express* **2011**, *19* (S3), A331−339. (b) Yu, H.; Deng, D.; Xu, S.; Yu, C.; Yin, H.; Nie, Q. L. *J. Lumin.* **2012**, *132*, 2553−2556. (c) Liu, C.; Xia, Z.; Lian, Z.; Zhou, J.; Yan, Q. *J. Mater. Chem. C* **2013**, *1*, 7139−7147.
(14) (a) Blasse, G.; Grabmaier, B. C. *Luminescent Materials;* SpringerVerlag: Berlin, Heidelberg, 1994. (b) Sun, J.; Sun, Y.; Zeng, J.; Du, H. *J. Phys. Chem. Solids* **2013**, *74*, 1007−1011. (c) Zhou, J.; Xia, Z.; Yang, M.; Shen, K. *J. Mater. Chem.* **2012**, *22*, 21935−21941.
(15) (a) Krevel, J. W. H.; Hintzen, H. T.; Metselaar, R.; Meijerink, A. *J. Alloys Compd.* **1998**, *268*, 272−277. (b) Zhang, Y.; Geng, D.; Shang, M.; Wu, Y.; Li, X.; Lian, H.; Cheng, Z.; Lin, J. *Eur. J. Inorg. Chem.* **2013**, 4389−4397. (c) Zhang, Y.; Hao, J.; Mak, C. L.; Wei, X. *Opt. Express* **2011**, *19*, 1824−1829.
(16) (a) Han, X. M.; Lin, J.; Zhou, H. L.; Yu, M.; Zhou, Y. H.; Pang, M. L. *J. Phys.: Condens. Matter* **2004**, *16*, 2745−2755. (b) Wen, D.; Shi, J. *Dalton Trans.* **2013**, *42*, 16621−16629. (c) Guo, C.; Jing, H.; Li, T. *RSC Adv.* **2012**, *2*, 2119−2122.
(17) (a) Sohn, K. S.; Choi, Y. Y.; Park, H. D.; Choi, Y. G. *J. Electrochem. Soc.* **2000**, *147*, 2375−2379. (b) Sohn, K. S.; Shin, N. *Electrochem. Solid-State Lett.* **2002**, *5*, H21−H23. (c) Geng, D.; Shang, M.; Zhang, Y.; Lian, H.; Lin, J. *Inorg. Chem.* **2013**, *52*, 13708−13718.
(18) Lu, W.; Hao, Z.; Zhang, X.; Luo, Y.; Wang, X.; Zhang, J. *Inorg. Chem.* **2011**, *50*, 7846−7851.
(19) (a) Blasse, G. *Philips Res. Rep.* **1969**, *24*, 131−136. (b) Xia, Z.; Liu, R. S.; Huang, K. W.; Drozd, V. *J. Mater. Chem.* **2012**, *22*, 15183−15189. (c) Jia, Y.; Qiao, H.; Zheng, Y.; Guo, N.; You, H. *Phys. Chem. Chem. Phys.* **2012**, *14*, 3537−3542.
(20) (a) Yang, W. J.; Chen, T. M. *Appl. Phys. Lett.* **2006**, *88*, 101903. (b) Kwon, K. H.; Im, W. B.; Jang, H. S.; Yoo, H. S.; Jeon, D. Y. *Inorg. Chem.* **2009**, *48*, 11525−11532. (c) Paulose, P. I.; Jose, G.; Thomas, V.; Unnikrishnan, N. V.; Warrier, M. K. R. *J. Phys. Chem. Solids* **2003**, *64*, 841−846. (d) Dexter, D. L. *J. Chem. Phys.* **1953**, *21*, 836−850.
(21) (a) Kuo, T. W.; Chen, T. M. *J. Electrochem. Soc.* **2010**, *157* (6), J216−J220. (b) Xia, Z.; Liu, R. S. *J. Phys. Chem. C* **2012**, *116*, 15604−15609. (c) Han, B.; Zhang, J.; Lu, Y. *J. Am. Ceram. Soc.* **2013**, *96* (1), 179−183.
(22) Liu, W. R.; Huang, C. H.; Wu, C. P.; Chiu, Y. C.; Yeh, Y. T.; Chen, T. M. *J. Mater. Chem.* **2011**, *21*, 6869−6874.
(23) Shang, M.; Geng, D.; Yang, D.; Kang, X.; Zhang, Y.; Lin, J. *Inorg. Chem.* **2013**, *52*, 3102−3112.